ChemMedChem

Chemistry Europe
European Chemical Societies Publishing

Accepted Article

Title: Bisubstrate ether-linked uridine-peptide conjugates as O-GlcNAc transferase inhibitors

Authors: Santosh Rudrawar, Vivek Makwana, Philip Ryan, Alpeshkumar K Malde, and Shailendra Anoopkumar-Dukie

To be cited as: *ChemMedChem* 10.1002/cmdc.202000582

Link to VoR: https://doi.org/10.1002/cmdc.202000582

WILEY-VCH

Bisubstrate ether-linked uridine-peptide conjugates as *O*-GlcNAc transferase inhibitors

Vivek Makwana[a,b,c], Dr Philip Ryan[a,b,c], Dr Alpeshkumar K Malde[d,e], A/Prof Shailendra Anoopkumar-Dukie[a,b,c], and Dr Santosh Rudrawar[a,b,c]*

Abstract: The *O*-linked β-*N*-acetylglucosamine (*O*-GlcNAc) transferase (OGT) is a master regulator of installing *O*-GlcNAc onto serine or threonine residues on a multitude of target proteins. Numerous nuclear and cytosolic proteins with varying functional classes including translational factors, transcription factors, signaling proteins, phosphate kinase are OGT substrates. Aberrant O-GlcNAcylation of proteins is implicated in signaling in metabolic diseases such as diabetes and cancer. The selective and potent OGT inhibitors are valuable tools to study the role of OGT in modulating a wide range of effects on cellular functions. We report linear bisubstrate ether-linked uridine-peptide conjugates as OGT inhibitors having micromolar affinity. *In vitro* evaluation of the compounds revealed the importance of donor substrate, linker and acceptor substrate in the rational design of bisubstrate analogue inhibitors. Molecular dynamics simulations shed light on the binding of this novel class of inhibitors and rationalized the effect of amino acid truncation of acceptor peptide on OGT inhibition.

Introduction

The *O*-linked *N*-acetylglucosamine (*O*-GlcNAc) post-translational protein modification (*O*-GlcNAcylation) is a dynamic and highly conserved process. The ubiquitously expressed *O*-GlcNAc transferase (OGT) catalyzes attachment of *O*-GlcNAc to serine and threonine residues of nucleocytoplasmic target proteins (**Figure 1**).[1] This process is reversed by the activity of another enzyme known as *O*-GlcNAcase (OGA) and balanced activity of these two enzymes tightly regulates *O*-GlcNAc cycle in cells. Deregulation of *O*-GlcNAcylation and elevated OGT enzyme levels are implicated in different metabolic disorders such as diabetes[2] and cancer[3-4] as well as on neurodegenerative diseases.[5] A plethora of evidence suggests immersion of OGT enzyme in cancer progression and metastasis *via* stabilization of various oncogenic factors such as c-MYC, HIF-1α and NF-κβ.[6-7] The inhibitor probes capable of monitoring enzymatic activity of OGT are important tools that may be used to gain better understanding on its precise role in pathology of various diseases.[8] The absence of potent, selective and cell permeable OGT inhibitors has hampered the development of this under-explored area and there is a dire need for such probes.[6]

[a] Menzies Health Institute Queensland, Griffith University, Gold Coast, QLD 4222, Australia.
[b] School of Pharmacy and Pharmacology, Griffith University, Gold Coast, QLD 4222, Australia. E-mail: s.rudrawar@griffith.edu.au
[c] Quality Use of Medicines Network, Griffith University, Gold Coast, QLD 4222, Australia.
[d] Institute for Glycomics, Griffith University, Gold Coast, QLD 4222, Australia.
[e] MaldE Scientific, https://maldescientific.com, Australia

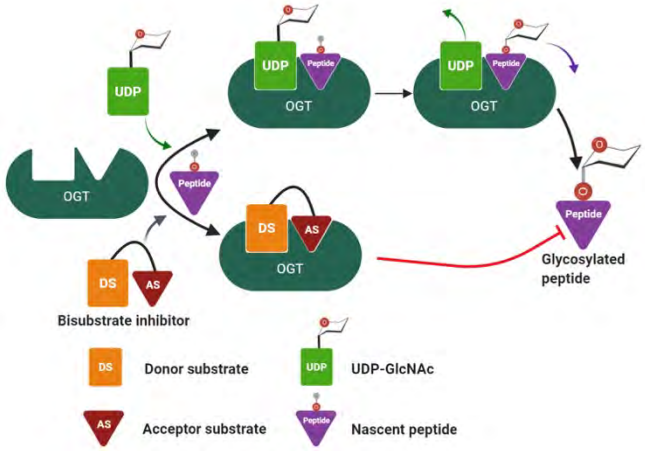

Figure 1. OGT catalyzed *O*-GlcNAcylation and bisubstrate analogue as OGT inhibitor.

OGT inhibitors could help to enrich our understanding of *O*-GlcNAcylation and help in the development of effective therapeutic strategies to target chronic conditions such as diabetes, cancer and neurodegenerative diseases.

The sugar donor substrate of OGT enzyme, UDP-GlcNAc, the by-product of *O*-GlcNAcylation UDP (IC_{50} = 1.8 μM) and various UDP-GlcNAc analogues such as, *C*-UDP (IC_{50} = 9 μM), UDP-*C*-GlcNAc (IC_{50} = 41 μM),[9a] UDP-*S*-GlcNAc (IC_{50} = 93 μM) were studied.[9b] A metabolic inhibitor, 5S-GlcNAc is introduced as OGT inhibitor from the class which is converted into donor substrate analogue UDP-5S-GlcNAc *in situ* by hijacking the hexosamine biosynthetic pathway, the metabolic pathway through which UDP-GlcNAc is biosynthesised.[10] Inhibitors related to the donor substrate, UDP-GlcNAc, in terms of structure or function, tend to exhibit poor selectivity for the enzyme target, along with poor cell permeability. UDP-GlcNAc is common substrate employed by many glycosyltransferase enzymes (*N*-acetylglucosaminyltransferase, *N*-acetylglucosamine-1-phosphotransferase,[11a] UDP-GalNAc-4-epimerase,[11b] UDP-GlcNAc-2-epimerase), hence its analogues lack selectivity.[11] Cell penetrance of such inhibitors is limited by the presence of the negatively charged pyrophosphate group. Non-substrate inhibitors ST045849 (IC_{50} = 53 μM), identified through high throughput screening[12a] and L01 (IC_{50} = 21.8 μM), identified through virtual screening[12b] are also described.[12] More recently OSMI-1 (IC_{50} = 2.7 μM) was reported as cell-permeable OGT

inhibitor, however its utility is limited due to negative impact on cell viability stemming from as it possesses off target effects.[12c] Furthermore, scaffold optimization based upon OSMI-1 resulted into development of the most potent OGT inhibitor, OSMI-4 (EC_{50} = 3 μM).[12g] Here we report, our progress towards development of bisubstrate analogues as OGT inhibitors.

Results and Discussion

Design

OGT being a bisubstrate enzyme, requires donor substrate as well as acceptor substrate to catalyze *O*-GlcNAcylation reaction. The concept of bisubstrate analogue inhibitors is a logical one and is a well-established strategy for development of inhibitors for glycosyltransferase enzymes.[13] Bisubstrate analogue inhibitors involve the covalent linkage of donor and acceptor substrates through linker.[14] The donor moiety provides affinity/potency whereas the acceptor provides selectivity.[13a] Use of a linker group allow proper orientation of donor and acceptor moieties toward optimum binding within the respective binding site(s) of the enzyme (**Figure 1**). Recently, bisubstrate analogue inhibitors of OGT have been reported following this basic structure. Goblin-1 (IC_{50} = 18 μM) is the first reported bisubstrate analogue inhibitor of OGT which contains UDP as donor part and heptapeptide (VTPVSTA) as an acceptor tethered by short linker.[15] Though it exhibited low-micromolar affinity for OGT enzyme *in vitro,* it failed to cross cell membrane due to presence of charged pyrophosphate moiety.[15] Cell penetrating peptides (CPPs) with fluorescent probes were introduced, and reasonably resolved the issue of cell permeability with traceability.[16] Despite having an inhibitory activity against hOGT enzyme in a cell free environment, it did not reduce global *O*-GlcNAcylation in HeLa cells as trapped in the early endosomes.[16] It was noted that the limited cell permeability caused by pyrophosphate moiety, was tempered by introducing CPP. Addition of CPP may reduce the selectivity preference of OGT enzyme for acceptor substrate. Also notable is that the K_d of UDP-GlcNAc (16 μM) is 32-fold higher than UDP (0.5 μM), highlighting that the presence of GlcNAc reduces the affinity towards the enzyme.[17] In our design, pyrophosphate is replaced with a neutral alkyl linker to connect uridine (donor substrate) and peptide (acceptor substrate) in linear fashion (**Figure 2**). To identify the minimum structural requirements for OGT inhibition we investigated AIPVSRAEK, VTPVSTA and STPVSSANM peptide sequences for use in inhibitor synthesis.[18] This is the first report, to the best of our knowledge, where an α-A crystallin derivative (AIPVSRAEK)[18a] has been employed as an acceptor substrate and where bisubstrate uridine-peptide conjugate assembled in a linear orientation. Most, if not all, of the reported bisubstrate OGT inhibitors such as Goblin-1, Thiogoblin, peptidic hybrids have exploited VTPVSTA sequence or its modification, linked *via* a centrally situated tether to peptide sequence.[12f,15-16] To evaluate efficiency of uridine as a donor substrate moiety, bisubstrate analogues containing GlcNAc as donor substrate moiety were designed as negative control. As the acceptor substrate is responsible for selectivity, attempts were made to minimize the length of peptide sequence to identify the minimum structural requirement of peptide sequence for OGT interaction.

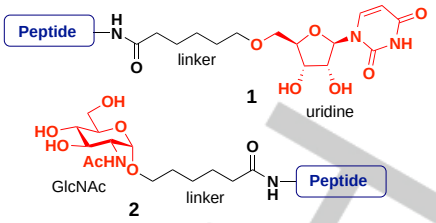

Figure 2. Proposed design of uridine (**1**) and GlcNAc (**2**) based bisubstrate analogous as OGT inhibitors.

Chemistry

The construction of envisaged ether linked bisubstrate conjugates (**1** and **2**) was initiated with synthesis of sugar donor analogues uridine-linker and GlcNAc-linker moieties. This synthetic strategy enables installation of tethered uridine/GlcNAc on a panel of peptide backbone on a solid support at the last synthetic phase.

Synthesis of ether-linked uridine derivative

To improve synthetic efficiency, the isopropylidene protected uridine **3** was synthesized from commercially available uridine in quantitative yields (SI).[19] The selection of an orthogonal acid labile protecting group could allow deprotection along with peptide sidechain protecting groups under resin cleavage conditions to afford the final uridine-peptide conjugates. The primary hydroxyl group (5′-hydroxyl) of acetonide **3** was alkylated with ethyl 6-bromohexanoate under basic condition to give ether-linked ester precursor **4** in quantitative yields (88%). Subsequent saponification of ethyl ester with sodium hydroxide (aq. 1M) resulted in uridine building block **5** in 87% yield (**Scheme 1**).

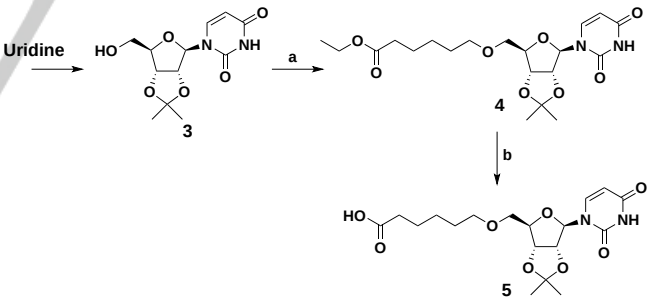

Scheme 1. Reagents and conditions: a) Ethyl 6-bromohexanoate, K_2CO_3, DMF, rt, 48 h, 88%; b) 1M NaOH (aq.), MeOH, rt, 3 h, 87%.

Synthesis of ether-linked GlcNAc derivative

The linker benzyl 6-hydroxyhexanoate was prepared from ε-caprolactone over two steps in 90% yield (SI).[20] *N*-Acetylglucosamine was reacted with acetyl chloride to afford glycosyl chloride **6** in 70% yield (SI).[21] The glycosylation reaction was carried with benzyl 6-hydroxyhexanoate under $ZnCl_2$ catalyzed condition[22] to afford α-glycoside **7** in 60% yield. Hydrogenolysis of the benzyl ester proceeded smoothly giving 60% crude yield of the ether-linked GlcNAc derivative **8** which did not require purification (**Scheme 2**).[23]

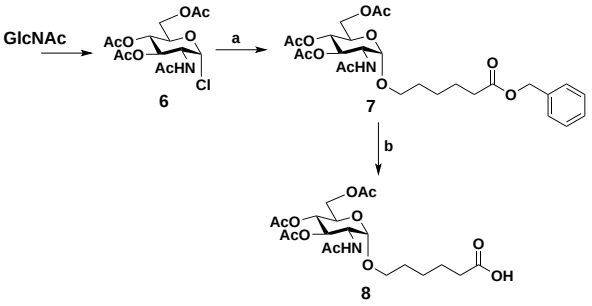

Scheme 2. Reagents and conditions: a) Benzyl 6-hydroxyhexanoate, $ZnCl_2$, DCM, rt, 24 h, 70%; b) H_2, Pd/C (wt %), MeOH, rt, 24 h, 60%.

Solid-phase synthesis of accepter substrate analogues

A well-characterised, high-affinity, acceptor substrate analogue is a vital component of a highly selective and potent bisubstrate inhibitor. The lack of a recognisable consensus motif made the selection of the acceptor peptide sequence for inhibitor design challenging. We opted for peptide sequences for which OGT binding is well-characterised. We selected bona fide OGT substrates α-A crystallin derived peptide AIPVSRAEK,[18a] retinoblastoma-like protein 2 (RBL-2) derived peptide VTPVSTA[18b] and casein kinase II (CK II) derived peptide STPVSSANM.[18c] To determine the minimum required length of peptide sequence for inhibition, truncated peptides [from -4 to -1 position (here S is considered as 0 position for numbering amino acid in peptide sequence)] of AIPVSRAEK were considered. After synthesis of donor analogues **5** and **8**, we focused on synthesis of the acceptor peptide substrate library using *N*-fluorenylmethoxycarbonyl based solid phase peptide synthesis (Fmoc-SPPS) using a Rink amide (AM) resin. Synthesis of the peptide began with the deprotection of Fmoc on Rink amide resin 555 mg/0.25 mmol (Loading capacity: 0.45 mmol/g) with piperidine in *N*,*N*-dimethylformamide (DMF 20% v/v) affording the primary amine, followed by loading with Fmoc-Lys(Boc)-OH in the case of α-A crystallin-derived peptides or Fmoc-Ala-OH for RBL-2 derived peptide or Fmoc-Met-OH for CK II derived peptide using *N*-methylmorpholine (NMM) as the base and benzotraizol-1-yl-oxytripyrrolidinophosphonium hexafluorophosphate (PyBOP) as the coupling reagent in DMF. Elongation of peptide sequence was conducted following Fmoc-SPPS strategy (**Scheme 3**).

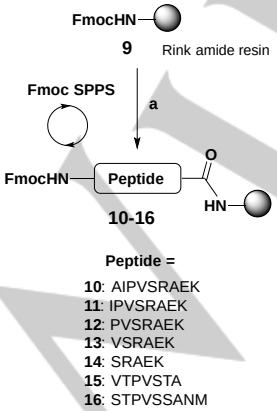

Scheme 3. Reagents and conditions: a) i) Fmoc deprotection: 20% piperidine/DMF; ii) Coupling: Fmoc-AA-OH (4eq), PyBOP (4eq), NMM (8 eq) in DMF; iii) Capping: 10% Ac_2O/pyridine

On-resin preparation of bisubstrate analogue conjugates

With all the building blocks in hand, we planned assembly of the ether linked uridine-peptide and GlcNAc-peptide conjugates on solid support. Synthesis was initiated by removing *N*-terminal Fmoc protecting group, followed by coupling of the donor analogues **5** or **8**. To improve synthetic efficiency, the reactive coupling reagent 2-(7-aza-1H-benzotriazole-1-yl)-1,1,3,3-tetramethyluronium hexafluorophosphate (HATU) was used. Additionally, the reactions were conducted over 24 h to ensure complete conjugation of the substrate analogous. Side chain deprotection and cleavage of conjugates from solid support using an acidic cocktail (90:5:5 TFA/TIS/H_2O) gave the desired ether linked uridine-peptide and GlcNAc-peptide conjugates in quantitative yields (70-85%) as determined by liquid chromatography-mass spectrometry (LC-MS) analysis. The conjugates were isolated by preparative reverse-phase high performance liquid chromatography (RP-HPLC) and formation is confirmed by high resolution mass spectrometry (HR-MS) (**Scheme 4**).

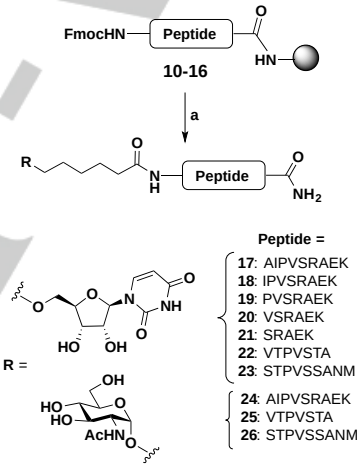

Scheme 4. Reagents and conditions: a) i) Fmoc deprotection: 20% piperidine/DMF; ii) Donor analogue coupling: one of **5** or **8** (1-2 eq), HATU (4 eq), NMM (8 eq), in DMF; iii) Resin cleavage: 90:5:5 TFA/TIS/H_2O, Et_2O wash, iii) **24**-**26** Acetate deprotection: NaOMe, MeOH, rt, 4 h, iv) Purification by RP-HPLC

Biological Evaluation

In vitro enzymatic activity

Following the successfully synthesis of a series of bisubstrate analogous, we screened OGT inhibitors. Inhibitory activity of compounds **17**-**26** was assessed against hOGT enzyme using UDP-Glo glycosyltransferase assay in which UDP, produced as a result of *O*-GlcNAc transfer to a peptide acceptor (CKII), is detected as an indication of glycosylation reaction.[12c] As shown in Table 1, compound **17** was identified as the most potent bisubstrate OGT inhibitor amongst synthesized compounds with an IC_{50} value of 29.37 μM which is comparable to L01 (IC_{50} = 21.8 μM)[12b] in terms of potency. As a positive control, commercial OGT inhibitor (OSMI-1) was also tested and its IC_{50} value was found out to be 1.69 μM (see **Figure 3A**). Compound **20** and **21** have also demonstrated inhibitory activity against OGT and their IC_{50} values were 273.4 and 330.9 μM respectively. The

remaining compounds (compound **18** and **22-26**) exhibited either no inhibitory effect or acted as OGT substrate instead as shown in **Figure 3B**. Amongst selected thee peptide sequences, only **10** displayed inhibitory activity when tethered to donor substrate *via* linker, highlighting that selection of peptide substrate sequence may have significant influence on the inhibitory activity of the inhibitor. Literature shows that VTPVSTA (**15**) in its modified version and more importantly in the branched orientation displayed inhibitory activity.[15] Here, **22** was found to be OGT substrate instead of inhibitor which might be due to the change in the orientation. IC_{50} data of compounds **17** and **24** demonstrated a negative impact on their inhibitory action despite both the compounds sharing structural similarities. As suspected, replacement of uridine with GlcNAc in the structure of bisubstrate inhibitors led to inactivity. Attempts to evaluate minimum effective length of the peptide sequence of **10** by its truncation. Reduction in the inhibitory action for the compounds **17-21** was observed when removing amino acids sequentially from the structure of the acceptor substrate (**10**, see **Scheme 3**) in spite of uridine being present as a donor substrate. Hence, intact nonamer peptide sequence (AIPVSRAEK) was identified as the most useful acceptor substrate analogue in the given structural design. Bisubstrate inhibitors are considered to be competitive substrates for UDP-GlcNAc, as with other substrate mimetic inhibitors such as Ac4-5S-GlcNAc and thus IC_{50} shift was determined by increasing UDP-GlcNAc concentration by 2.5 folds. Results suggested that there was a clear shift in IC_{50} (see **Figure 3C**) which was as expected and proved that compound **17** is also a competitive inhibitor with respect to UDP-GlcNAc and has similar mode of inhibition. Then, time dependent inhibition of OGT was carried out to understand onset and duration of action for compound **17** (**Figure 3D**). Compound **17** exhibited lag phase of 10-15 min and achieved its maximum inhibition at 30 min (S17 and Table S1 provides further information on time dependent changes in IC_{50} values of compound **17** and OSMI-1). A further drop in the inhibitory action might be considered either due to weak binding capabilities or competitive displacement on time course. Although we have shown here that replacement of pyrophosphate with an aliphatic linker is able to allow evaluation of the compounds' abilities to permeate the cell membrane is still yet to be conducted.

Table 1. Inhibition of OGT enzyme with bisubstrate analogue inhibitors

Conjugates	IC_{50} (μM)	Hill Slope
17	29.37	-0.7882
18	52.48	1.829
19	ND	ND
20	273.4	-0.8482
21	330.9	-1.827
22	136.7	0.8488
23	81.31	1.232
24	ND	ND
25	33.53	1.608
26	ND	ND

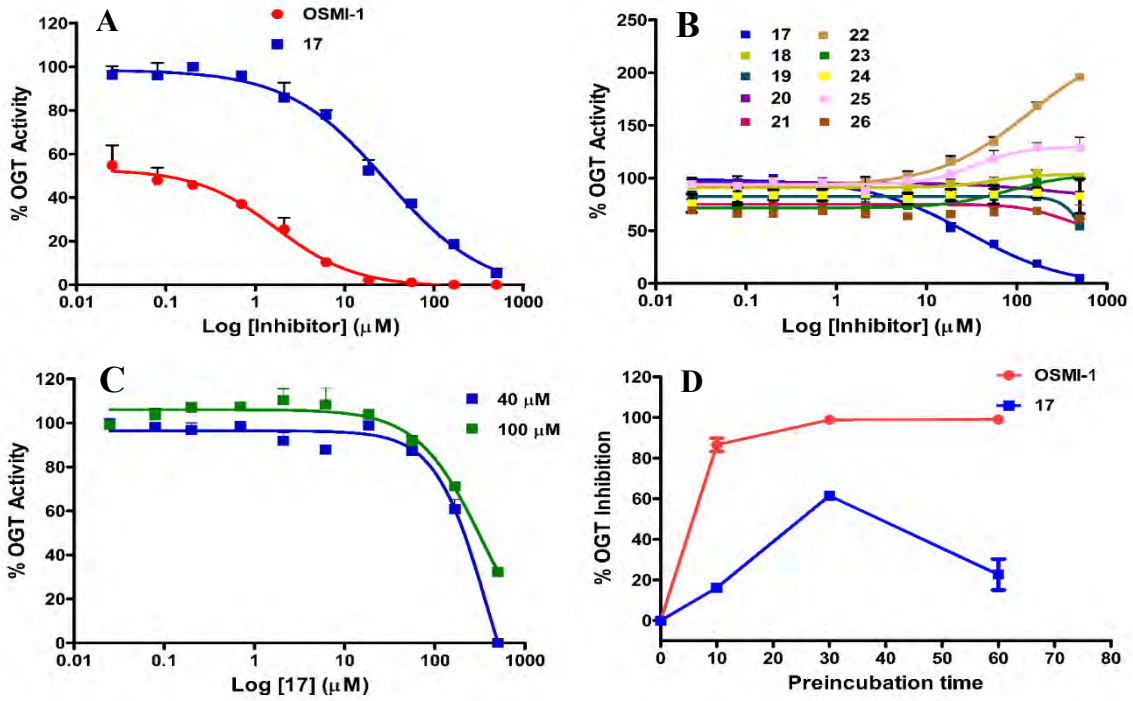

Figure 3. *In-vitro* inhibition of OGT enzyme by OSMI-1 and compound **17-26**. (A and B) Comparison of OGT inhibition activity of compounds **17-26** in a dose-dependent manner in the range of 0.025-500 μM using UDP-Glo assay. Glycosylation reaction was carried out at 40 μM UDP-GlcNAc and 125 μM peptide substrate (CKII3K) (data represent the mean ± SD, n=3). (C) IC_{50} shift by change in UDP-GlcNAc concentration (40 and 100 μM) determined using UDP-Glo assay (data represent the mean ± SD, n=3). (D) Time-dependent inhibition of OGT enzyme using UDP-Glo assay (data represent the mean ± SD, n=3). IC_{50} values are reported as averages obtained from three independent duplicate analysis (n = 3) of each compound.

ADME in silico predictions of the physicochemical and pharmacokinetic parameters of Globlin-1, Thiogoblin, peptide hybrid, alloxan, OSMI-1 and compound **17** were calculated using SwissADME server (http://www.swissadme.ch/).[24] The compound **17** shows increased LogP value which indicates that it might have more cell-permeability as compared to Goblin-1 and Thiogoblin theoretically (SI **Table S2**).

Molecular Dynamics (MD) Simulations

To understand the binding and interactions of **17**, the most potent inhibitor with the negative Hill slope, with human OGT, Molecular Dynamics Simulations (MD) were performed. Overlay of available human OGT crystal structures (**Figure S4**) indicated that the substrate peptide backbones occupy the same position in the binding pocket irrespective of its sequence and presence/absence of UDP, pyrophosphate, GlcNAc and whether peptide is linked to the cofactor. Based on this knowledge, we built the structure of inhibitor **17** by modifying the bound CK-2 peptide in the crystal structure of OGT in complex with UDP and a glycopeptide(PDB: 4GYW)[25] and adding the linker to connect Ala1 to uridine. Two independent 100 ns MD simulations revealed that the overall protein structure is stable in the simulation, while inhibitor **17** conformation fluctuates to adopt an optimal bound state as shown by the RMSD plot in Figure 4. The final bound conformation of **17** is shown in **Figure 5** and compared to the pseudo-Michalis complex in the crystal structure of OGT in complex with UDP-5S-GlcNAc and substrate peptide RB2L (PDB: 5C1D).[18b] The amino acids in **17** occupy the similar locations in the binding pocket as the peptide in 5C1D structure. However, the location of Uridine moiety is shifted to accommodate the linker connecting to the peptide. As opposed to the reported structural data on thio-linked UDP-peptide conjugates where inhibitor seems to adopt "U"-shaped conformation,[16] inhibitor **17** with a unique linker and no pyrophosphate adopts "O"-shaped conformation upon binding to OGT. Truncating the amino acids (inhibitors **18** to **21**) would shift either the Uridine moiety or peptide significantly in the binding pocket, and thus would lead to a systematic loss of inhibitory activity as observed experimentally (**Table 1**).

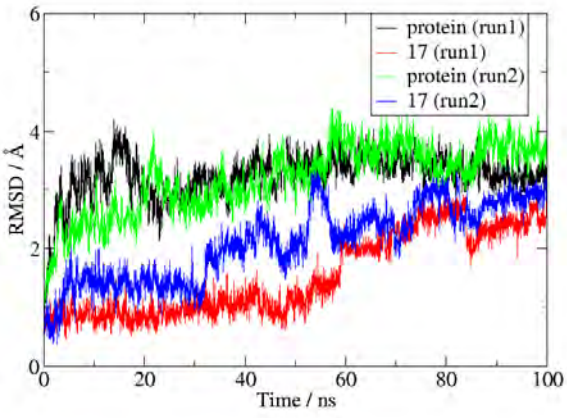

Figure 4. Atom-positional root-mean-square deviations (RMSDs) of the backbone atoms (Cα, N, C) in black/green and ligand atoms in red/blue from two independent 100 ns Molecular Dynamics simulations of OGT:**17** complex. The RMSD of the protein indicates that protein structure is stable. The ligand re-arranges in the binding pocket and stabilizes over 100 ns of simulations.

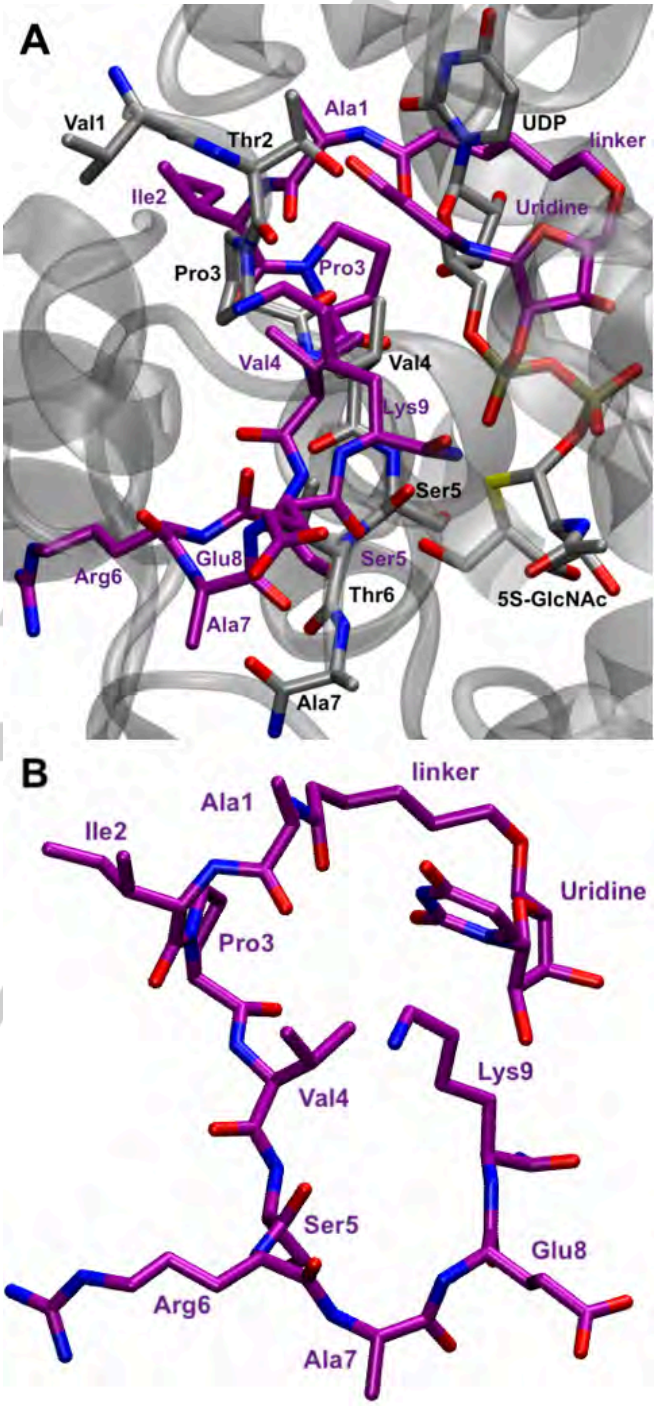

Figure 5. Predicted mode of binding of bisubstrate inhibitor (**17**) in OGT binding site (A) The binding of **17** (purple) to OGT as observed from MD simulations. The ligand seems to adopt O-shaped conformation in the binding pocket. The bound conformation (grey) of the peptide (VTPVSTA), UDP-5S-GlcNAc from the pseudo-Michaelis complex (PDB: 5C1D) is shown. Inhibitor **17** occupies the same binding pocket and first five amino acid residues occupy the same region. Uridine moiety in **17** is realigned to accommodate the ether linker. (B) An alternate view of the bound conformation of **17** indicating O-shaped binding is shown.

In future, further optimization of the scaffold might be initiated by changing the length of linker or linker type and replacing substrate

sequence with unmodifiable Sert to Ala mutants. There is also a possibility that derivativatization of donor part especially C_5-position with heterocyclic ring might increase lipophilicity of scaffold and hence improvement in cell permeability as well as binding affinity. This process might provide further information to understand structure activity relationship with OGT enzyme. Peptide delivery systems such as liposomes might serve as a vehicle to transport bisubstrate inhibitors without modifying its basic structure in a condition of complete lack of scope in chemical structure modification.

Conclusion

In conclusion, a potential bisubstrate inhibitor of OGT enzyme, **17** was rationally designed, synthesized, and found to possess OGT inhibitory activity in micro-molar scale (IC_{50} = 29.37 μM). Molecular dynamics simulations revealed that **17** has opted "O-shaped" conformation upon binding to OGT enzyme. It also showed competitive inhibition with increasing concentrations of UDP-GlcNAc which suggested that it occupies UDP-binding pocket in OGT enzyme and is probable mode of action. This research work also evaluated tolerance of donor and acceptor in the basic structure of bisubstrate inhibitors and concludes that improper alignment of donor and acceptor results in loss of activity. Uridine was found to be more effective than GlcNAc in the design of UDP-GlcNAc analogue based inhibitors, as was the intact sequence of α-A-crystallin derivative (AIPVSRAEK), relative to its truncated analogues. Finally, we have shown that pyrophosphate is able to be replaced with a flexible linker allowing compounds to orient properly at binding site, besides potentially enhancing cell-permeability.

Experimental Section

Full experimental details are disclosed in the Supporting Information.

Acknowledgements

Financial support to SR from an Australian Research Council – Discovery Early Career Research Award (DE140101632) is gratefully acknowledged. SR expresses his sincere gratitude to Prof Richard J. Payne and Prof Kate Jolliffe (The University of Sydney) for their support. VM is supported by the Griffith University International Postgraduate Research Scholarship (GUIPRS) and the Griffith University Postgraduate Research Scholarship (GUPRS). Authors thank Jasmine Karanjia (University of South Australia) for proofreading and assistance with creating graphics. The computational work was funded with the assistance of high-performance computing resources provided through the National Computational Merit Allocation Scheme supported by the Australian Government (Project cj47) and Queensland Cyber Infrastructure Foundation (QCIF, Project fi49).

Keywords: Post-translational modification, OGT enzyme, *O*-GlcNAcylation, Bisubstrate inhibitors, Donor substrate, Acceptor substrate.

References

[1] L. Wells, K. Vosseller, G.W. Hart, *Science* **2001**, *291*, 2376.
[2] J. Ma, G.W. Hart, Expert Rev. Proteomic. **2013**, *10*, 365.
[3] J.P. Singh, K. Zhang, J. Wu, X. Yang, Cancer Lett. **2015**, *356*, 244.
[4] C.M. Ferrer, V.L. Sodi, M.J. Reginato, *J. Mol. Biol.* **2016**, *428*, 3282.
[5] W.B. Dias, G.W. Hart, *Mol. BioSyst.* **2007**, *3*, 766.
[6] V. Makwana, P. Ryan, B. Patel, S. Anoopkumar-Dukie, S. Rudrawar, *Biochim. Biophys. Acta Gen. Subj.* **2019**, *1863*, 1302.
[7] Z. Ma, K. Vosseller, *J. Biol. Chem.* **2014**, *289*, 34457.
[8] R. Trapannone, K. Rafie, D.M. van Aalten, *Biochem. Soc. Trans.* **2016**, *44*, 88.
[9] a) H.C. Dorfmueller, V.S. Borodkin, D.E. Blair, S. Pathak, I. Navratilova, D.M. van Aalten, *Amino Acids* **2011**, *40*, 781; b) A.J. Clarke, R. Hurtado-Guerrero, S. Pathak, A. W. Schüttelkopf, V. Borodkin, S. M. Shepherd, A. F. Ibrahim, D. M. van Aalten, *EMBO J.* **2008**, *27*, 2780.
[10] T.M. Gloster, W.F. Zandberg, J.E. Heinonen, D.L. Shen, L. Deng, D.J. Vocadlo, *Nat. Chem. Biol.* **2011**, *7*, 174.
[11] a) Y. Qian, H. Flanagan-Street, E. van Meel, R. Street, S.A. Kornfeld, PNAS, **2013**, *110*, 10246; b) K. A. Winans, C. R. Bertozzi, *Chemistry & Biology* **2002**, *9*, 113.
[12] a) B.J. Gross, B.C. Kraybill, S. Walker, *J. Am. Chem. Soc.* **2005**, *127*, 14588; b) Y. Liu, Y. Ren, Y. Cao, H. Huang, Q. Wu, W. Li, S. Wu, J. Zhang, *Sci. Rep.* **2017**, *7*, 12334; c) R.F. Ortiz-Meoz, J. Jiang, M.B. Lazarus, M. Orman, J. Janetzko, C. Fan, D.Y. Du- veau, Z.-W. Tan, C.J. Thomas, S. Walker, *ACS Chem. Biol.* **2015**, *10*, 1392; d) S. Wang, D. L. Shen, D. Lafont, A.-S. Vercoutter-Edouart, M. Mortuaire, Y. Shi, O. Maniti, A. Girard-Egrot, T. Lefebvre, B. Mario Pinto, D. Vocadlo, S. Vidal, *Med. Chem. Commun.* 2014, 5, 1172; e) Y. Wang, J. Zhu, L. Zhang, J. Med. Chem. 2016, 60, 263; f) H. Zhang, T. Tommšič, J. Shi, M. Weiss, R. Ruijtenbeek, M. Anderluh, R.J. Pieters, *Med. Chem. Commun.* 2018, 9, 883; g) S.E.S. Martin, Z.-W. Tan, H.M. Itkonen, D.Y. Duveau, J.A. Paulo, J. Janetzko, P.L. Boutz, L. Törk, F.A. Moss, C.J. Thomas, S.P. Gygi, M.B. Lazarus, S. Walker, *J. Am. Chem. Soc.* **2018**, *140*, 13542.
[13] a) M. Izumi, H. Yuasa, H. Hashimoto, *Curr. Top. Med. Chem.* **2009**, *9*, 87; b) L. L. Lairson, B. Henrissat, G. J. Davies, S. G. Withers, *Annu. Rev. Biochem.* **2008**, *77*, 521.
[14] D. Lavogina, E. Enkvist, A. Uri, *ChemMedChem*. **2010**, *5*, 23.
[15] V.S. Borodkin, M. Schimpl, M. Gundogdu, K. Rafie, H.C. Dorfmueller, D.A. Robinson, D.M. van Aalten, Biochem. J. **2014**, *457*, 497.
[16] K. Rafie, A. Gorelik, R. Trapannone, V.S. Borodkin, D.M. van Aalten, *Bioconjug. Chem.* **2018**, *29*, 1834.
[17] M. Schimpl, X. Zheng, V.S. Borodkin, D.E. Blair, A.T. Ferenbach, A.W. Schüttelkopf, I. Navratilova, T. Aristotelous, O. Albarbarawi, D.A. Robinson, *Nat. Chem. Biol.* **2012**, *8*, 969.
[18] a) T.M. Leavy, C.R. Bertozzi, *Bioorg. Med. Chem. Lett.* **2007**, *17*, 3851; b) S. Pathak, J. Alonso, M. Schimpl, K. Rafie, D.E. Blair, V.S. Borodkin, O. Albarbarawi, D.M. van Aalten, *Nat. Str. Mol. Biol.* **2015**, *22*, 744; c) M.B. Lazarua, Y. Nam, J. Jiang, P. Sliz, S. Walker, *Nature* **2011**, *469*, 564.
[19] M. Tiecco, P.D. Profio, R. Germani, G. Savelli, *Nucleos. Nucleot. Nucl.* **2009**, *28*, 911.
[20] S.W. Svenningsen, A. Janaszewska, M. Ficker, J.F. Petersen, B. Klajnert-Maculewicz, J.B. Christensen, *Bioconjug. Chem.* **2016**, *27*, 1547.
[21] D. Horton, M. Wolfrom, *J. Org. Chem.* **1962**, *27*, 1794.
[22] Y. Meng, Y. Guo, Y. Ling, Y. Zhao, Q. Zhang, X. Zhou, F. Ding, Y. Yang, *Bioorg. Med. Chem.* **2011**, *19*, 5577.
[23] G. Kinberger, T. Prakash, J. Yu, G. Vasquez, A. Low, A. Chappell, K. Schmidt, H. Murray, H. Gaus, E. Swayze, *Bioorg. Med. Chem. Lett.* **2016**, *26*, 3690.
[24] A. Daina, O. Michielin, V. Zoete, *Sci. Rep.* **2017**, *7*, 42717.
[25] M.B. Lazarus, J. Jiang, T.M. Gloster, W.F. Zandberg, G.E. Whitworth, D.J. Vocadlo, S. Walker, *Nat. Chem. Biol.* **2012**, *8*, 966.

Graphical abstract